UDC 577.32

HOMOLOGY MODELING AND MOLECULAR DYNAMICS STUDY OF *MYCOBACTERIUM TUBERCULOSIS* UREASE

Lisnyak Yu. V., Martynov A. V.

SI "I. Mechnikov Institute of Microbiology and Imunology of National Academy of Medical Sciences of Ukraine"

Introduction

Mycobacterium tuberculosis, the causative agent of tuberculosis, infects approximately one third of the world's population and kills almost 2 million people every year [1]. Although it is frequently proposed that vaccination is the most effective way to combat tuberculosis, numerous attempts to develop more efficacious vaccines than available ones have failed [2]. Thus, new anti-tuberculosis drugs are urgently needed. One of the potential targets for chemotherapeutic intervention in tuberculosis is *M. tuberculosis* urease (MTU).

Urease, a nickel-containing enzyme (urea amidohydrolase, EC 3.5.1.5) [3-6], is produced by various bacteria [7-17], fungi [8, 18], and plants [7, 8, 19-21]. Within past two decades bacterial ureases have gained much attention in research field as a virulence factor in human and animal infections [7, 8, 17, 22-24], and, correspondingly, as an attractive target for designing new safe and efficient enzyme inhibitors aimed to combat infectious diseases stipulated by urease activity [25-34]. A prerequisite for designing such inhibitors is an understanding of urease's three-dimensional (3D) structure organization.

Plant and fungal ureases are homo-oligomeric proteins, while bacterial ureases are multimers of three-subunits (except *Helicobacter pylori* which comprises two-subunits). Despite these differences, bacterial and plant ureases are gomologous, and have a similar three-dimensional structure (fig. 1) and conservative catalytic mechanism [6, 7, 35, 36]. Three sub-units of bacterial ureases, UreC (α-chain), UreB (β-chain), and UreA (γ-chain), form a T-shaped heterotrimer αβγ (fig. 1). Three αβγ heterotrimers form quaternary complex $(\alpha\beta\gamma)_3$, homotrimer of heterotrimers. Active center is located in α-domain and contains two atoms of nickel coordinated by carboxylated lysine, aspartic acid and histidine

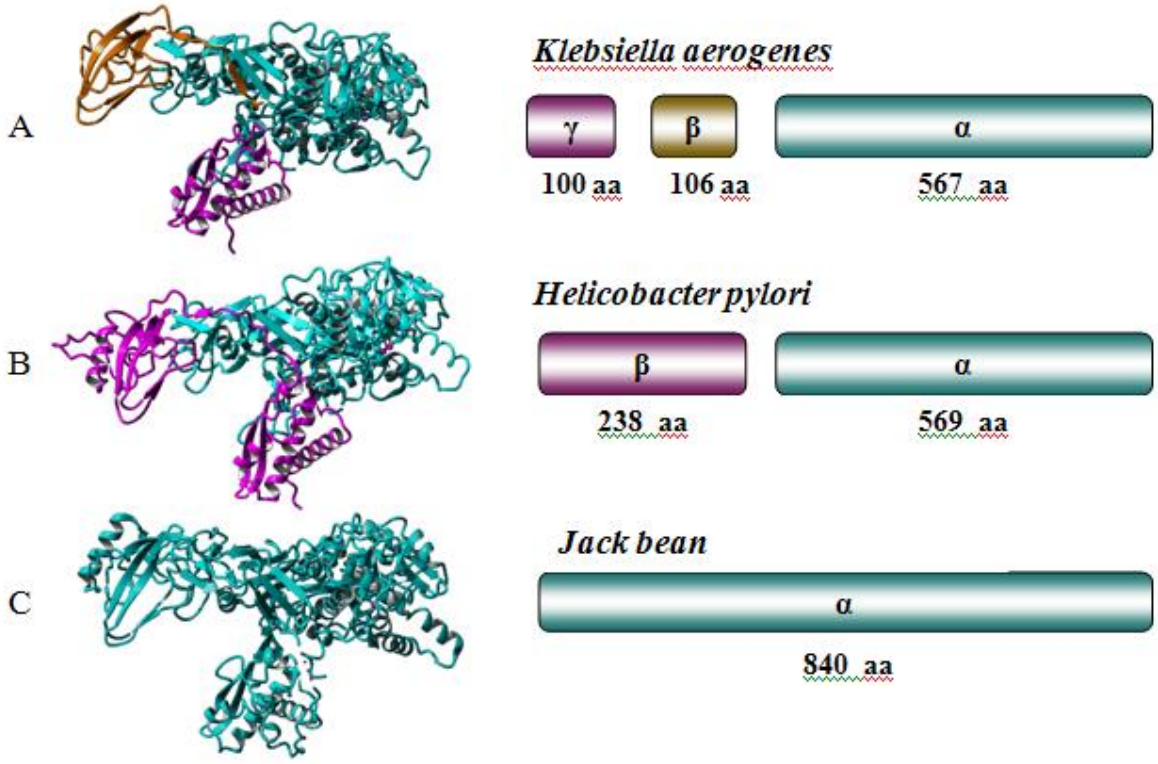

Fig. 1. – Sub-unit organization and X-ray structure of bacterial and plant ureases. A – characteristic bacterial urease, *Klebsiella aerogenes* urease, consisting of three sub-units: α (cyan), β (gold) and γ (lilac) (PDB code 2KAU). B –*Helicobacter pylori* urease consisting of two sub-units: α (cyan) and β (lilac) (PDB code 1E9Z). C – characteristic eukariotic urease, jack bean urease, represented by a single α (cyan) unit (PDB code 1E9Z).

DOI: 10.5281/zenodo.1000132

residues. Active site is capped by a flap that controls substrate ingress to and product egress from the dinickel center. Amongst bacterial ureases, only X-ray structures of the enzymes from *Helicobacter pylori*, *Klebsiella aerogenes*, and
Sporosarcina pasteurii (formerly known as *Bacillus pasteurii*) have been determined till now [37-40]. Three-dimensional structure of *M. tuberculosis* urease is unknown. X-ray structure has been determined only for its γ sub-unit, which unlike α and β sub-units has no known enzymatic functions and supposed to serve as a scaffold for the urease quaternary complex $(\alpha\beta\gamma)_3$ [41]. When experimental three-dimensional structure of a protein is not known, homology modeling, the most commonly used computational structure prediction method, is the technique of choice [42-44]. This paper aimed to build a 3D-structure of *M. tuberculosis* urease by homology modeling and to study its stability by molecular dynamics simulations.

Materials and methods

***Homology modeling*.** The target amino acid sequence of *Mycobacterium tuberculosis* H37Rv urease was retrieved from GenBank at NCBI : α-chain (UreC), 100 amino acid residues (Accession AAC3707.01, GJ:886331); β-chain (UreB), 104 amino acid residues (Accession AAC37006.1, GJ:886330), and γ-chain (UreA), 577 amino acid residues (Accession AAC37005.1, GJ:886329) [45]. Potential modeling templates were identified by runninig PSI-BLAST [46, 47] to extract a position-specific scoring matrix from UniRef90 and then searching the PDB [48] for a match with the target sequence. The templates were ranked based on the alignment score and the structural quality according to WHAT_CHECK [49] obtained from the PDBFinder2 database[50]. Amongst the top-scoring templates, five high-resolution X-ray structures were selected for *Klebsiella aerogenes*, *Sporosarcina pasteurii*, and *Enterobacter aerogenes* bacterial ureases with three-subunit composition: 2KAU, 5G4H, 4UBP, 4CEU, and 4EPB. The template's amino acid sequence identity with the target was within 56.9% - 59.1%. For each template five stochastic alignments were created [51] using SSALIGN scoring matrices [52]. Then for each alignment, a three-dimensional model was built using loop conformation extracted from the PDB [53] and the SCRWL side-chain placement algorithm [54]. Hydrogen bonding network was optimized [55]. Each model was energy minimized with explicit water molecules using Yasara2 force field [56], and the models were ranked by quality Z-score. The best scoring model was further refined by running a 500 ps molecular dynamics simulation using Yasara2 force field. During the simulation, snapshots were saved every 25 ps and rated according to the quality Z-score. The model with highest quality score was chosen as a final homology model of 3D structure for *M. tuberculosis* urease.

Homology model building, refining, validation, molecular dynamics simulations, and analysis as well as the result presentation by using molecular graphics were done by molecular modeling program YASARA Structure [55-61]. Additionaly, the final model was validated by using QMEAN [62-64], PDBsum [65-70], and PISA [71] servers.

***Molecular dynamics*.** MTU trimer αβγ was placed in a cubic periodic cell filled with TIP3P water molecules. The simulation cell was 1 nm larger than the trimer complex along all three axes. Na^+ and Cl^- counterions were added to neutralize the system and to reach ion mass fraction 0.9% NaCl [59]. The system was energy-minimized using AMBER14 force field [72] with a 1.05 nm force cutoff for dispersion interactions. To treat longrange electrostatic interactions the Particle Mesh Ewald algorithm [73] was used. After a short steepest descent minimization, the procedure continued by simulated annealing minimization. The molecular dynamics simulations were run in NPT ensemble at 300 K and pH 7.4 using a multiple timestep of 2.5 fs for intra-molecular and 5 fs for inter-molecular forces [61]. Trajectory was computed for 60 ns

Results and discussion

Homology model of Mycobacterium tuberculosis urease. Homology model of MTU is a nonamer (homotrimer of heterotrimers, $(\alpha\beta\gamma)_3$) consisting of 2349 residues (fig. 2). To build MTU model, five high-resolution X-ray structures of bacterial ureases with three-subunit composition (2KAU, 5G4H, 4UBP, 4CEU, and 4EPB) have been selected as templates. For each template five stochastic alignments were created and for each alignment, a three-dimensional model was built. Then, each model was energy minimized and the models were ranked by quality Z-score. A quality Z-score estimates the quality of a model in relation to experimental high- resolution X-ray structures. Z-score is normalized to mean 0

DOI: 10.5281/zenodo.1000132

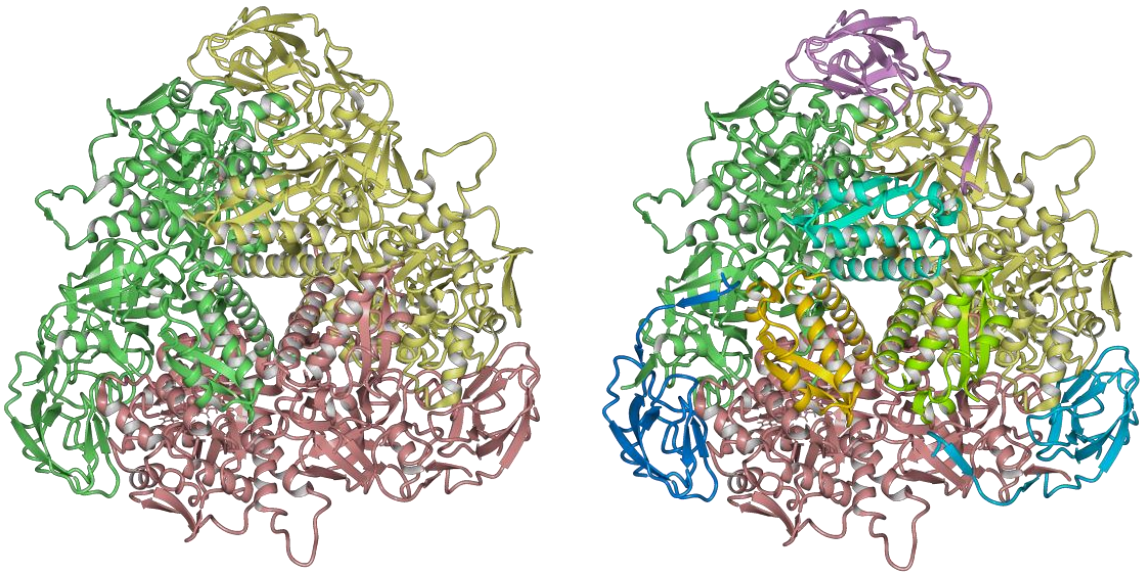

A B

Fig. 2 – 3D model of *M. tuberculosis* urease. A – homotrimer of heterotrimers $(\alpha\beta\gamma)_3$. The homotrimers are differently colored. B – sub-unit structure of the homotrimer of heterotrimers $(\alpha\beta\gamma)_3$. In each heterotrimer, α, β and γ sub-units are differently colored.

and standard deviation 1 and indicates how many standard deviations the model differs from values for experimental structures. Z-scores form the basis of most structure validation tools. The Yasara's quality Z-score based on knowledge-based dihedral angle and packing potentials is weighted sum of 'Dihedrals', 'Packing1D' and 'Packing3D' contributions [56]. The MTU model with highest quality estimation amongst 25 potential models was selected. To further improve structure quality the model was refined by short molecular dynamics simulation that resulted in 20 snapshots which were rated according to their energy and the quality Z-score. The best scoring model having minimum energy was chosen as a final homology model of 3D structure for *M. tuberculosis*. Fig. 3 shows MTU heterotrimer αβγ colored according to per-residue Z-score values.

The model of MTU was also validated by using PDBsum and QMEAN servers. Ramachandran plots for MTU heterotrimer and homotrimer of heterotrimers are shown in fig. 4.

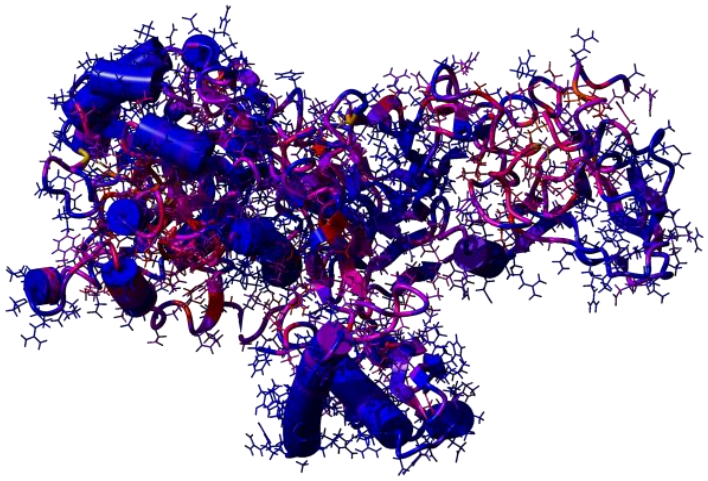

Fig. 3 – MTU heterotrimer αβγ colored according to per-residue Z-score values. Colors range from yellow (bad/incorrect) to blue (perfect/correct).

In heterotrimer (fig. 4A), 90.2%, 8.7%, 0.9%, and 0.2% of total residues are present in the most favored, additional allowed, generously allowed, and disallowed regions, respectively. In homotrimer of heterotrimers (fig. 4B), 90.1%, 8.5%, 1.0%, and 0.4% of total residues are present, respectively, in the most favored, additional allowed, generously allowed, and disallowed regions.

QMEAN Z-score estimates an absolute quality of a protein structure by relating the model's structural

DOI: 10.5281/zenodo.1000132

features to experimental structures of similar size. The QMEAN's scoring function is a weighted linear combination of four statistical potential terms (torsion, pairwise C_β, all-atom interactions and solvation) and two additional terms describing the agreement of the predicted and observed secondary structure, and solvent accessibility [62-63]. Fig. 5 shows QMEAN score of MTU model compared to the experimental structures of similar size from PDB. The MTU (query model) score is colored in red. Fig. 6 represents density plot of all

A

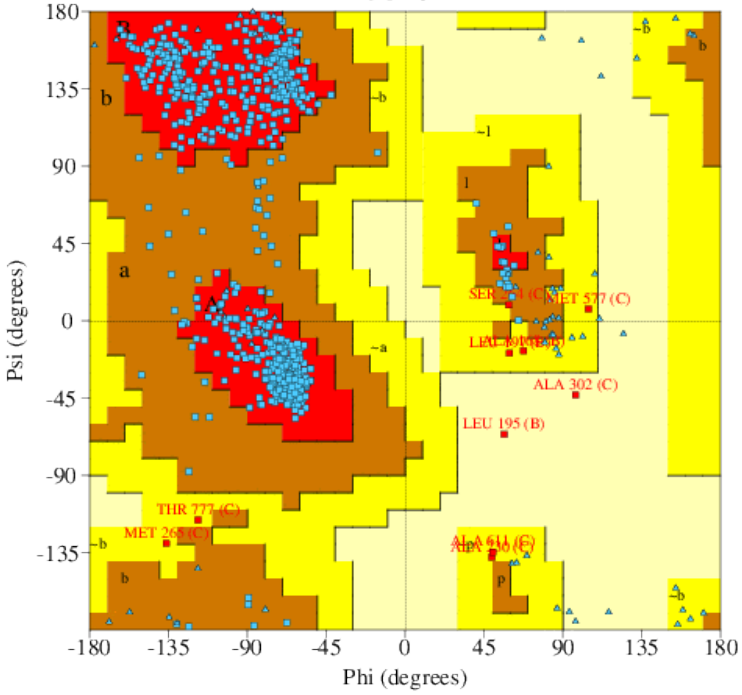

B

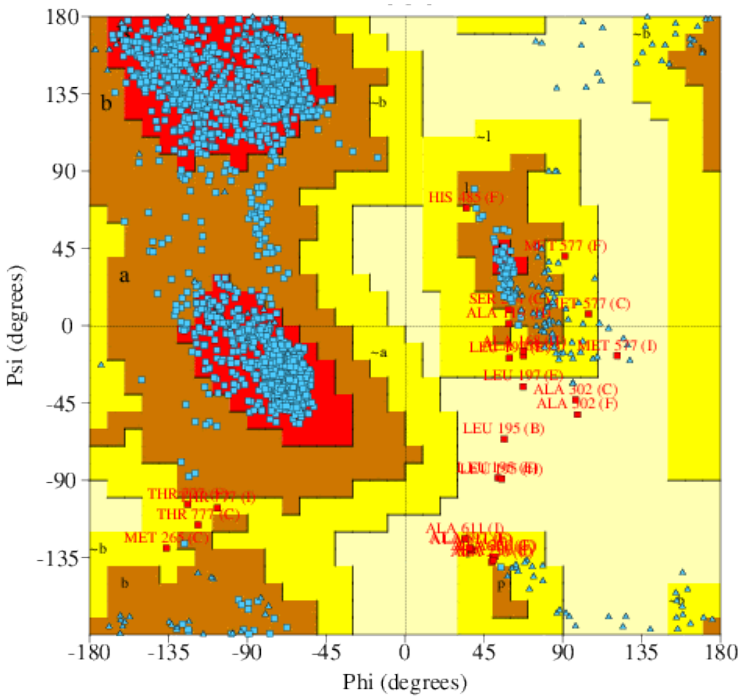

Fig. 4. - Ramachandran plots for MTU heterotrimer (A) and homotrimer of heterotrimers (B). (Generated from PDBsum server).

DOI: 10.5281/zenodo.1000132

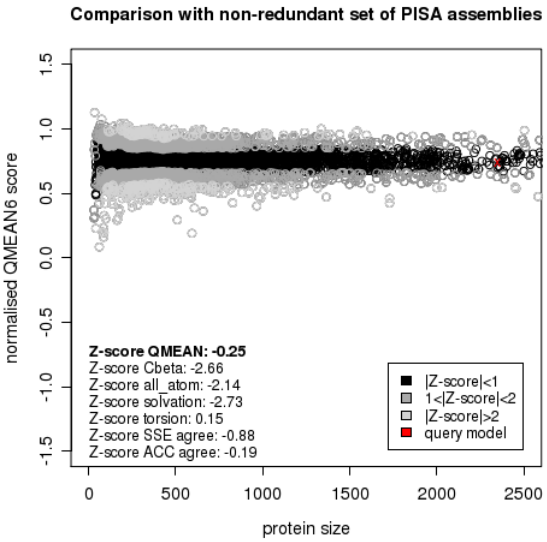

Fig. 5 – QMEAN score of MTU compared to the experimental structures of similar size from the PDB. (Generated from QMEAN server.)

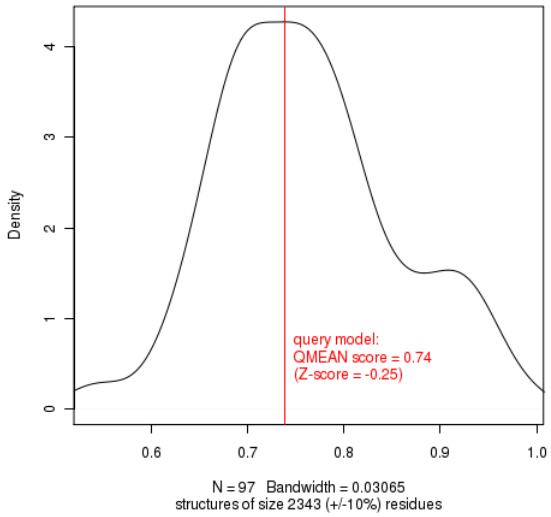

Fig. 6 – Density plot of all reference models used in the Z-score calculation. The location of MTU model ("query model") with regard to the background distribution is marked in red. The number of reference models used in the calculation is shown under the plot. (Generated from QMEAN server.)

reference models used in the Z-score calculation as well as the location of MTU model (marked in red). Thus, above structure validations confirm good quality of our homology model of *M. tuberculosis* urease.

In *M. tuberculosis* urease heterotrimer, sub-units α, β, and γ tightly interact with each other at a surface of approximately 3000 Å^2. Secondary structure of sub-units γ, β, and α is shown in fig. 7A, B and C, respectively. Topological scheme of mutual arrangement of the secondary structure elements in these sub-units is presented in figs. 8 and 9.

Sub-unit α contains the enzyme active site with two Ni atoms coordinated by amino acid residues His347, His349, carbamylated Lys430*, His459, His485, Asp 573, Gly490 (fig. 10). Helix-turn-helix motif (residues 524-545) forms a mobile flap that covers the active site (fig. 11A). The flap of bacterial ureases have been shown to exist in closed, open and wide-open conformations, respectively closing, opening and wide-opening access to the active site, and thus playing a key role in the control of urease activity [74-76]. In our model, the flap is in closed conformation impeding access to the enzyme active site (fig. 11B).

Molecular dynamics study of M. tuberculosis urease. The structural stability of our homology model was checked by molecular dynamics simulation of MTU in explicit water at 300 K and pH 7,4. During the simulation, root mean square deviations of C_α atoms (RMSD C_α) and root mean square fluctuations (RMSF) of amino acid residues of MTU were monitored for 60 ns. As can be seen from fig.12, after equilibration (beyond 20 ns) RMSD C_α values change insignificantly evidencing that MTU global structure is quite stable.

Analysis of RMSF values for individual amino acid residues of MTU, especially ones for its α sub-unit, reveals their different mobility (fig. 13). The highest fluctuations are observed in the regions covering residues Gly598-Asp612 and Asn520-Arg549. Residues of the first region form a loop situated at the periphery of the enzyme and supposed to be involved in intermolecular interactions between the apoenzyme and the accessory proteins that form the supercomplex that is necessary for the incorporation of the Ni ions at the active site and for the consequent urease activation [35, 74-77]. The other region corresponds to helix-turn-helix motif which forms a flap that covers the active site and modulates the enzyme activity [78-80], and thus is of the most interest for our analysis. In our model, the flap was in closed conformation.

To study the possible movement of this loop in relation to the active center (i.e. its potential for opening) there was monitored the distance between loop center and dinickel center for 60 ns. As can be seen from fig. 14, the distance between the loop and Ni atoms fluctuates in time around its average value 15.7 Å

DOI: 10.5281/zenodo.1000132

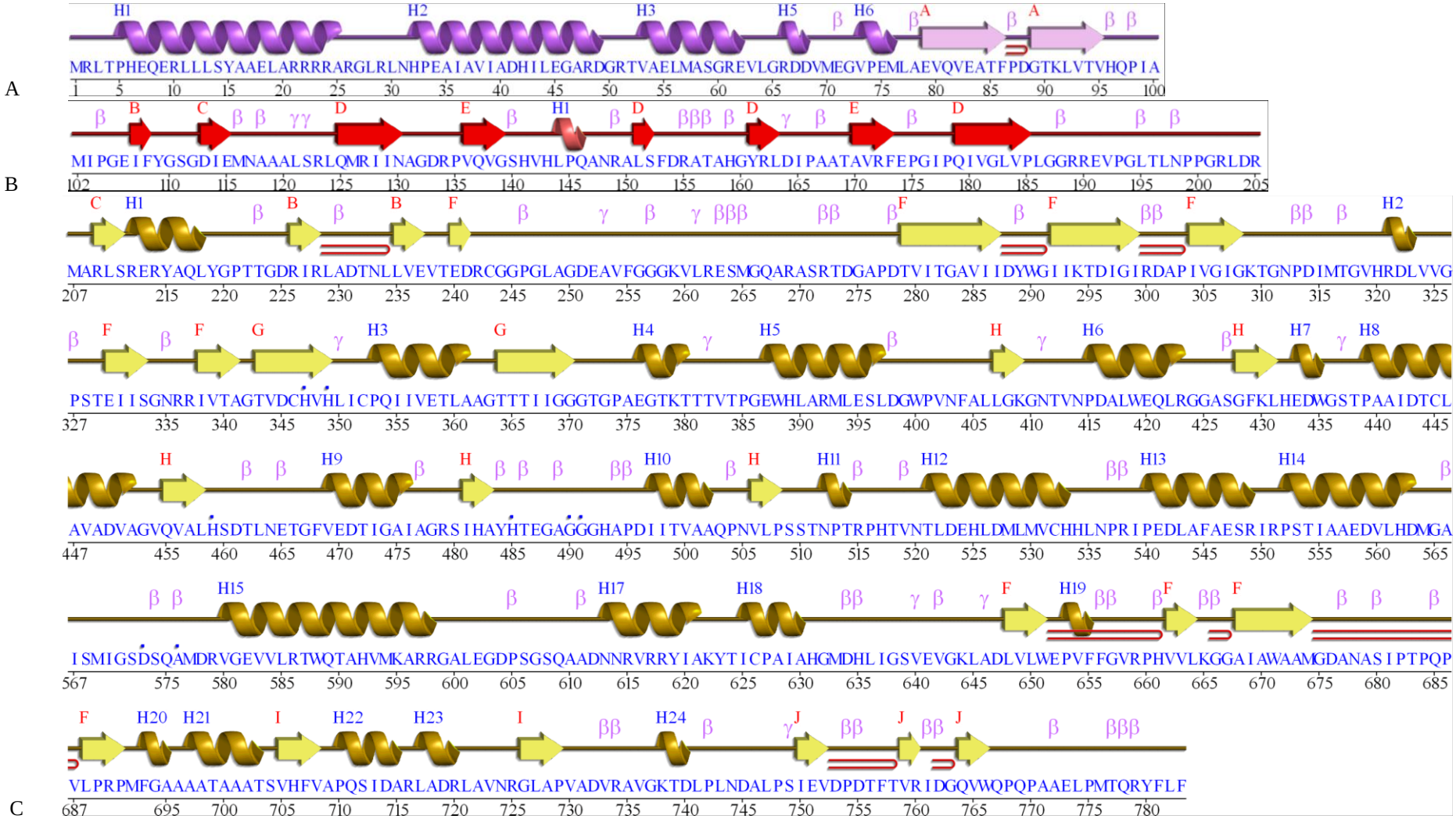

Fig. 7 – Secondary structure of *M. tuberculosis* urease. A, B and C represent γ, β and α subunits, correspondingly. (Generated from PDBsum server).

DOI: 10.5281/zenodo.1000132

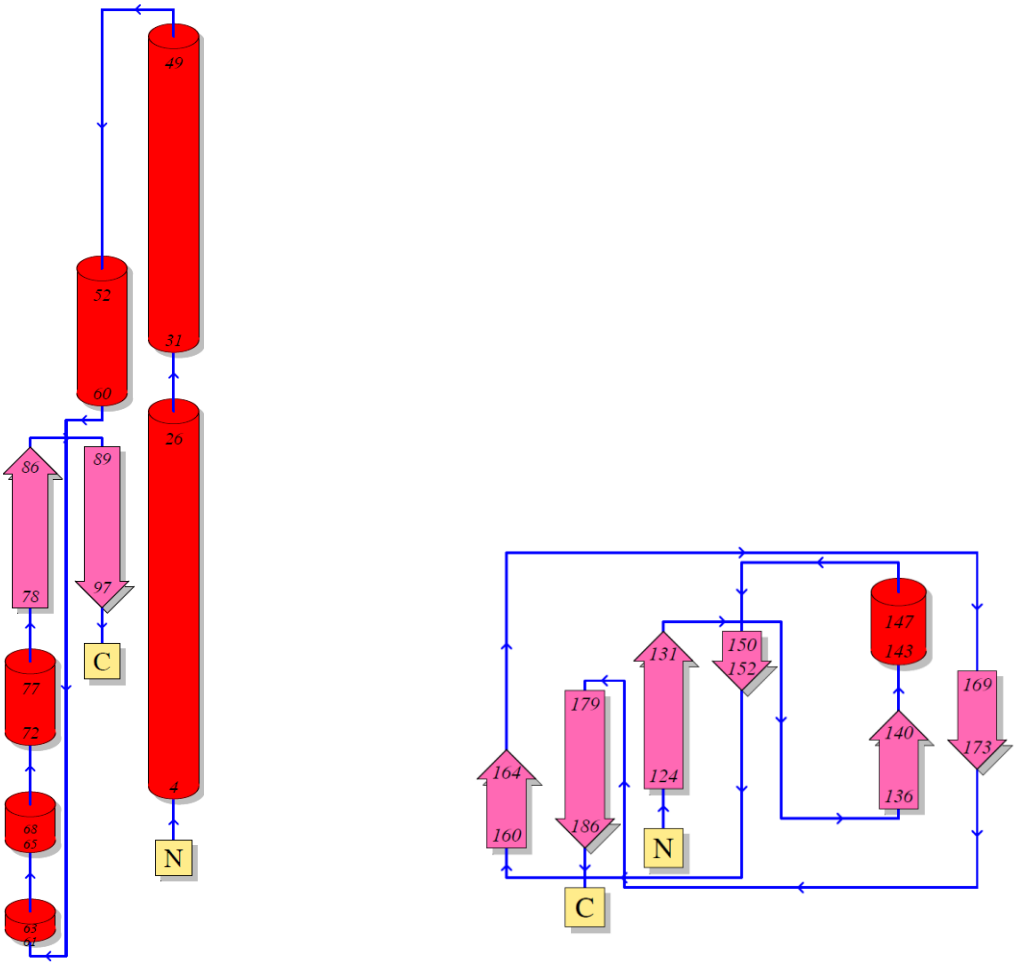

Fig. 8 – The topology diagram of the secondary structure elements in γ (left) and β (right) sub-units of *M. tuberculosis* urease. The large pink arrows are beta strands, the red cylinders are alpha-helices. The small blue arrows indicate the directionality of the protein chain. The numbers within the secondary structural elements correspond to the first and the last residue numbers. (Generated from PDBsum server.)

DOI: 10.5281/zenodo.1000132

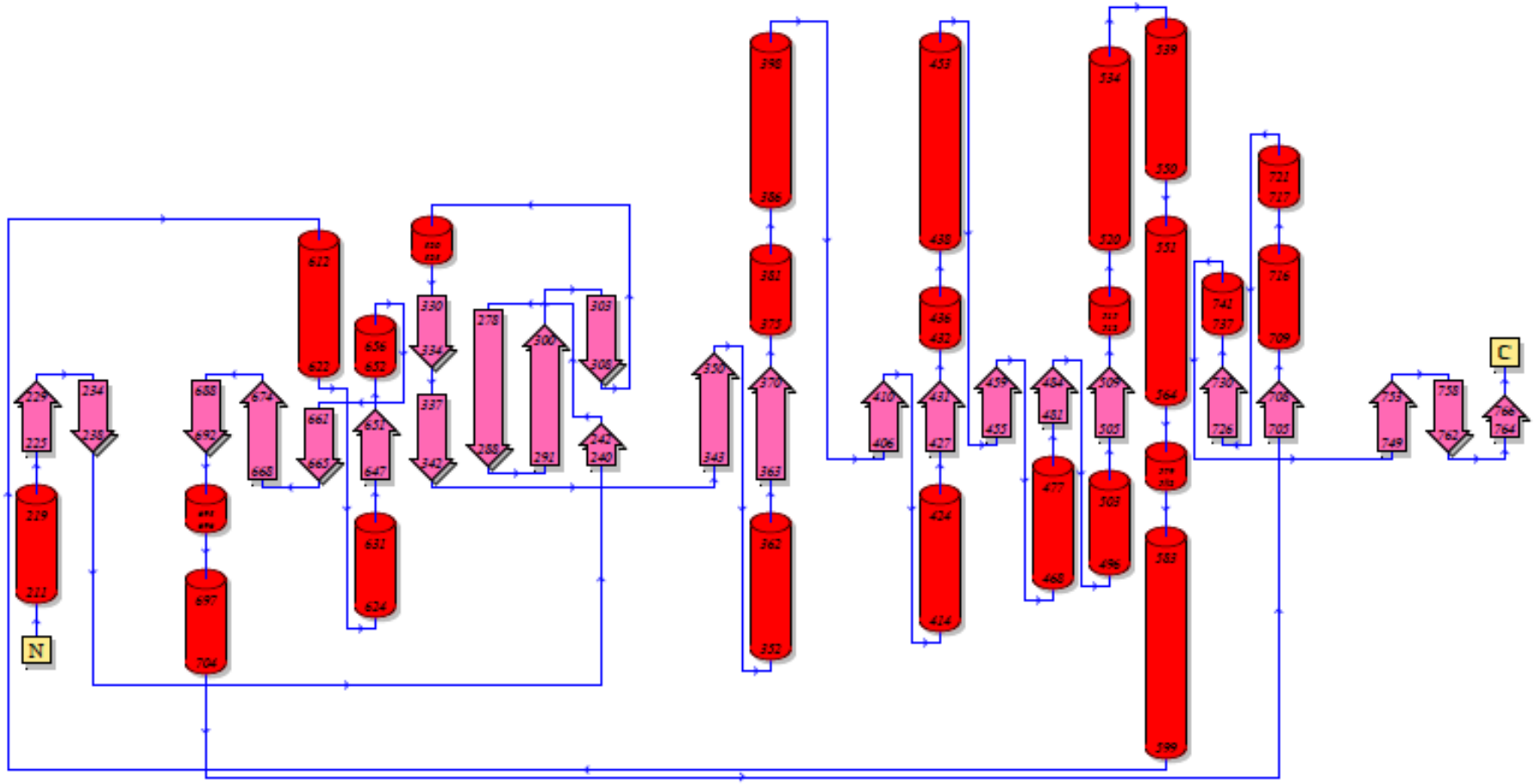

Fig. 9 –The topology diagram of mutual arrangement of the secondary structure elements in *M. tuberculosis* urease α sub-unit. The large pink arrows denote beta strands, the red cylinders denote alpha-helices. The small blue arrows indicate the directionality of the protein chain. The numbers within the secondary structural elements correspond to the first and the last residue numbers. (Generated from PDBsum server.)

DOI: 10.5281/zenodo.1000132

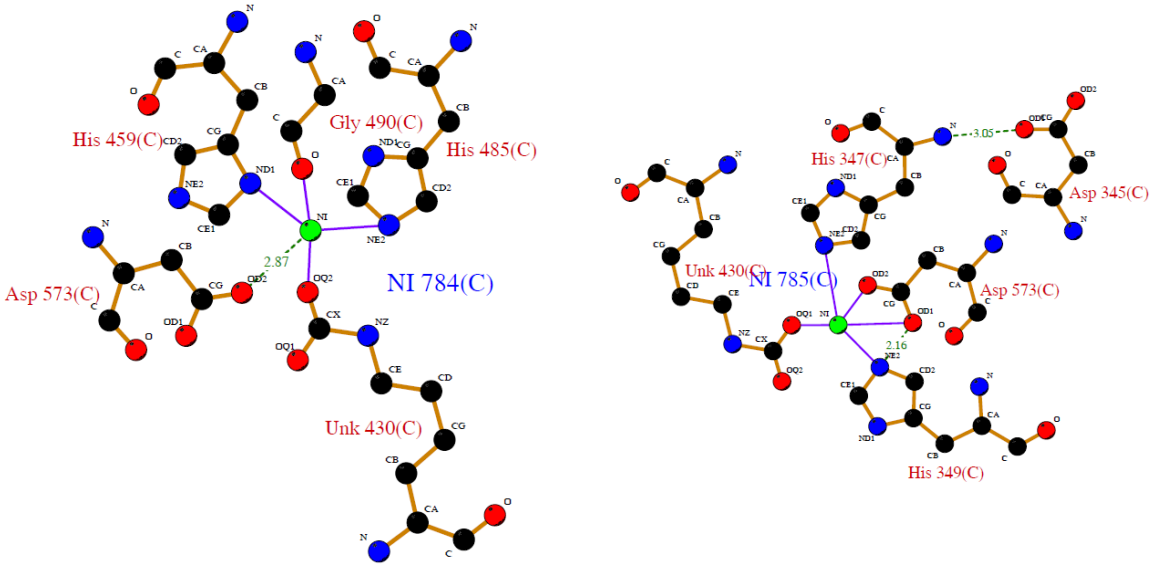

Fig. 10 - Nickel-protein interactions in the active site. Nickels, carbons, oxygens, and nitrogens are colored in green, black, red, and blue, respectively. Unk430 denotes carbamylated Lys430*. (Generated from PDBsum server).

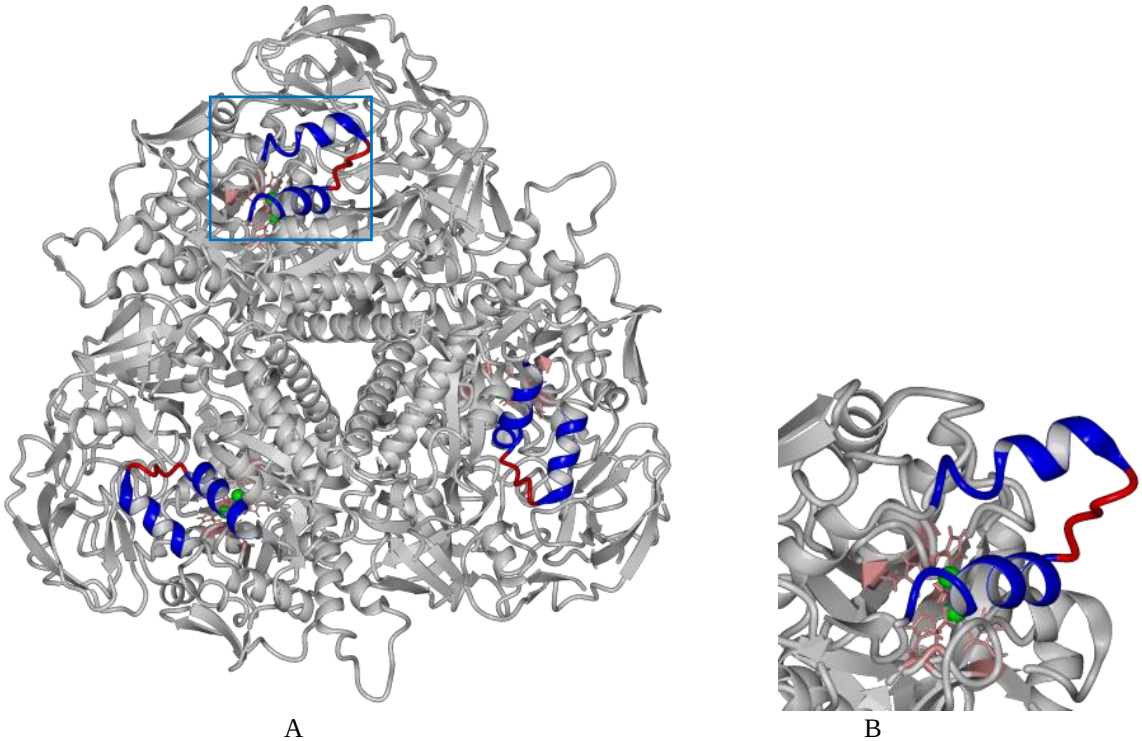

A B

Fig. 11 – The flap (helix–turn–helix motif) covering the active-site cleft. A – homotrimer of heterotrimers. B – Enlarged active site region of α sub-unit. Helixes and turns are colored in blue and red, Ni atoms and the active-site residues are shown in green and pink, correspondingly.

DOI: 10.5281/zenodo.1000132

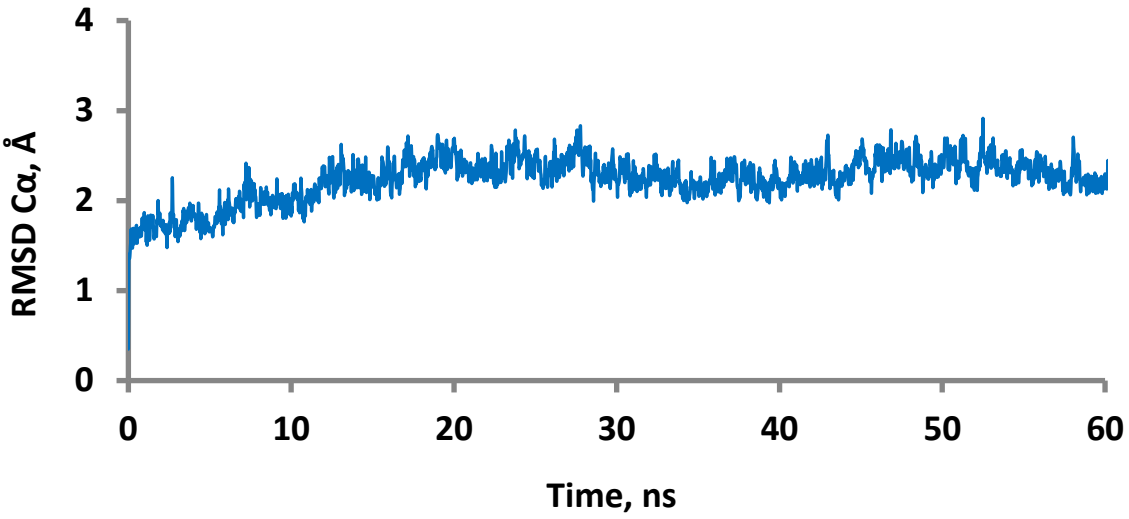

Fig. 12 – Root mean square deviations of C_α atoms (RMSD C_α) of MTU in dependence on simulation time.

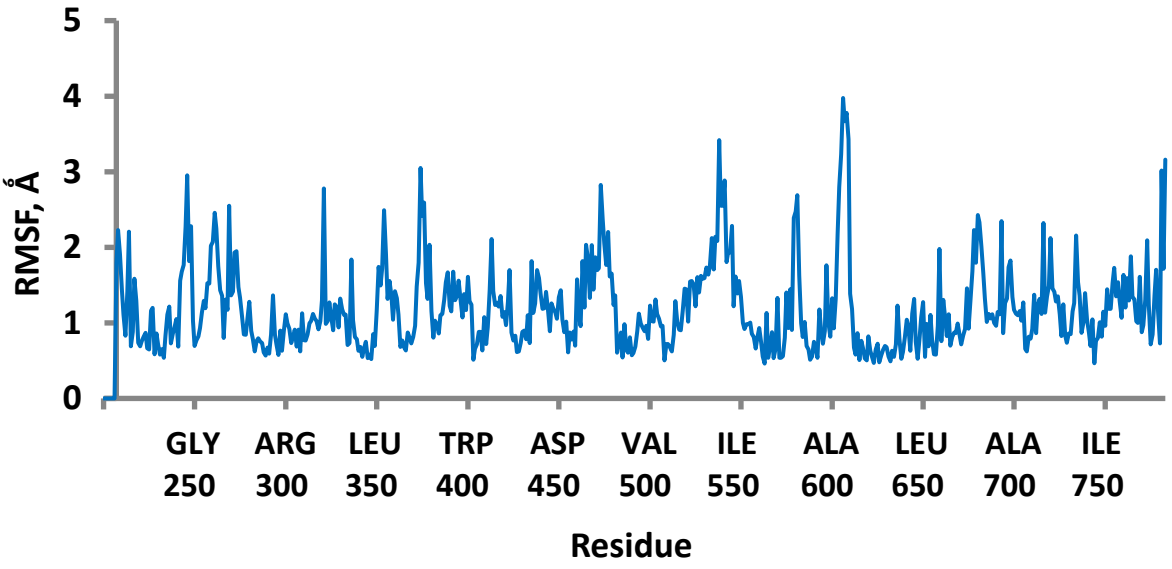

Fig. 13 – Root mean square fluctuations (RMSF) of α sub-unit amino acid residues of MTU.

DOI: 10.5281/zenodo.1000132

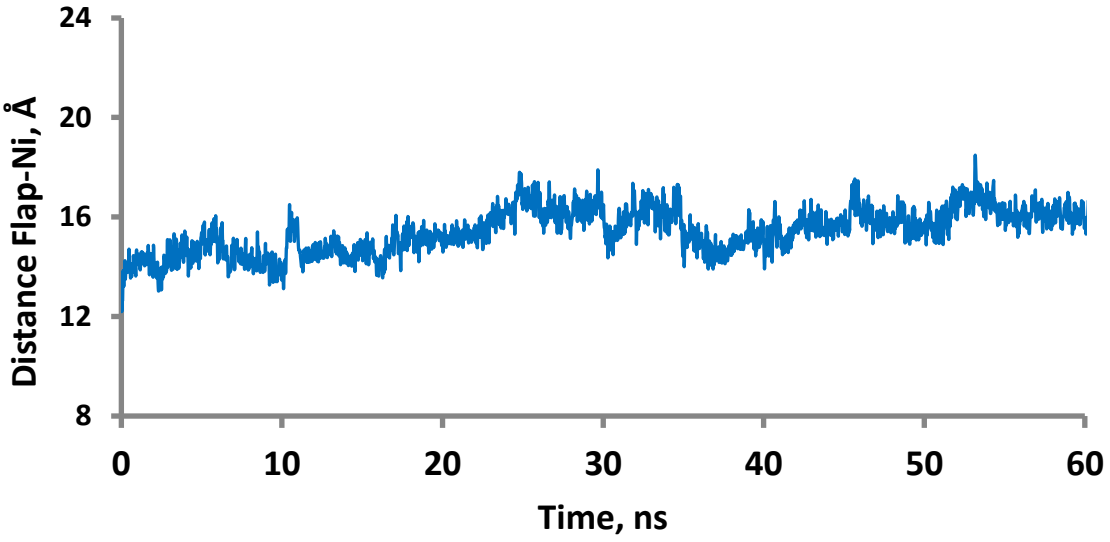

Fig. 14 – Distance between the flap center and the middle of a straight line connecting Ni atoms in the active center of MTU.

with low amplitude indicating that flap remains in closed state blocking an access to the active center. Recently, similar dynamic behavior of the flap in closed state was observed by Minkara M.S. et al. during the molecular dynamics simulation of *Helicobacter pylori* urease for 400 ns [81].

Taken together, the revealed structural features of 3D model of *M. tuberculosis* urease suggest that the overall structure of the enzyme is stable.

Conclusions

In this study three-dimensional structure of *M. tuberculosis* urease has been predicted by homology modeling. Thorough structure validations by alternative algorithms confirmed good quality of our homology model of *M. tuberculosis* urease. The structural stability of the model and the pecularities of the dynamic behavoir of its flap covering the active center was studied by molecular dynamics simulation of MTU in aqueous solution at 300 K for 60 ns. Analysis of MD trajectory indicate that the enzyme global structure is stable and the flap covering the active center remains in closed state during the simulation time. Predicted three-dimensional structure of *M. tuberculosis* urease can be used in the studies of structure-function relationships of the enzyme, in design of new safe and efficient enzyme inhibitors aimed to struggle with infectious diseases promoted by urease activity.

References

1. WHO/HTM/TB2010.7 Pn. WHO Report 2010: Global Tuberculosis Control. Geneva, Switzerland: WHO Press; 2010.
2. Cole, S. T. Inhibiting *Mycobacterium tuberculosis* within and without. Phil. Trans. R. Soc. B. – 2016. – Vol. 371: 20150506.
3. Dixon, N. E. 1975. Jack bean urease (EC 3.5.1.5). A metalloenzyme. A simple biological role for nickel? [Text] / N. E. Dixon, C. Gazzola, R. L. Blakeley, B. Zerner. // J. Am. Chem. Soc. – 1975. – Vol. 97. – P. 4131–4133.
4. Ragsdale, S. W. Nickel-based enzyme systems [Text] / S.W. Ragsdale // J. Biol. Chem. – 2009. – Vol. 284, N 28. – P. 18571–18575.
5. Carter, E. L. Interplay of metal ions and urease [Text] / E. L. Carter, N. Flugga, J. L. Boer, S. B. Mulrooney, R. P. Hausinger // Metallomics. – 2009. – Vol. 1. – P. 207-221.
6. Boer, J. L. Nickel-dependent metalloenzymes [Text] / J. L. Boer, S. B. Mulrooney, R. P. Hausinger // Arch. Biochem. Biophys. – 2014. – Vol. 544. – P. 142-152.
7. Mobley, H. L. T. Molecular biology of microbial ureases [Text] / H. T. Mobley, M. D. Island, R. P. Hausinger // Microbiol. Rev. – 1995. – Vol. 59, N 3. - P. 451–480.
8. Mobley, H. L. T. Microbial ureases: significance, regulation, and molecular characterization [Text] / H. L. T. Mobley, R. P. Hausinger // Microbiol. Rev. – 1989. – Vol. 53, N 1. – P. 85–108.
9. Suzuki, K. Urease-producing species of intestinal anaerobes and their activities [Text] / K. Suzuki, Y. Benno, T. Mitsuoka, S. Takebe, K. Kobashi, J. Hase // Appl. Environ. Microb. - 1979. – Vol. 37, N 3. - P. 379-382.
10. Murchan, S. Emergence, spread, and characterization of phage variants of epidemic methicillin-resistant *Staphylococcus aureus* 16 in England and Wales [Text] / S. Murchan, H. M. Aucken, G. L. O'Neill,.M. Ganner, B. D. Cookson // J. Clin. Microbiol. – 2004. – Vol. 42, N 11. – P. 5154-5160.
11. Jin, M. Development of a large-scale HPLC-based purification for the urease from *Staphylococcus leei* and determination of subunit structure [Text] / M. Jin, W. Rosario, E. Watler, D.H. Calhoun // Protein Expr. Purif. – 2004. – Vol. 34, N 1. – P. 111-117.
12. Clemens, D. L. Purification, characterization, and genetic analysis of *Mycobacterium tuberculosis* urease, a potentially critical determinant of host-pathogen interaction [Text] / D. L. Clemens, B.-Y. Lee, M. A.

DOI: 10.5281/zenodo.1000132

Horwitz // J. Bacteriol. – 1995. – Vol. 177, N 19. – P. 5644-5652.
13. Dupuy, B. *Clostridium perfringens* urease genes are plasmid borne [Text] / B. Dupuy, G. Daube, M. R. Popoff, S. T. Cole // Infect. Immun. – 1997. – Vol. 65, N 6. – P. 2313-2320.
14. Futagami, S. Systemic and local immune responses against *Helicobacter pylori* urease in patients with chronic gastritis: distinct IgA and IgG productive sites [Text] / S. Futagami, H. Takahashi, Y. Norose, M. Kobayashi, M. // Gut. – 1998. – Vol. 43, N 2. – P. 168-175.
15. Nakano, M. Association of the urease gene with enterohemorrhagic *Escherichia coli* strains irrespective of their serogroups [Text] / M. Nakano, T. Iida, M. Ohnishi, K. Kurokawa, A. Takahashi, T. Tsukamoto, T. Yasunaga, T. Hayashi, T. Honda // J. Clin. Microbiol. – 2001. – Vol. 39, N 12. – P. 4541-4543.
16. Orth, D. Prevalence, structure and expression of urease genes in Shiga toxin-producing *Escherichia coli* from humans and the environment [Text] / D. Orth, K. Grif, M. P. Dierich, R. Wurzner // Int. J. Hyg. Environ.-Health. – 2006. – Vol. 209, N 6. – P. 513-520.
17. Konieczna, I. Bacterial ureases and its role in long-lasting human diseases [Text] / I. Konieczna, P. Zarnowiec, M. Kwinkowski, et al. // Curr. Protein. Pept. Sci. – 2012. – Vol. 13. – P. 789-806.
18. Tange, Y. Identification of the ure1+ gene encoding urease in fission yeast [Text] / Y. Tange, O. Niwa // Curr. Genet. – 1997. – Vol. 32, N 3. – P. 244-246.
19. Sirko, A. Plant ureases: roles and regulation [Text] / A. Sirko, R. Brodzik // Acta Biochim. Pol. – 2000. – Vol. 47, N 4. – P. 1189-1195.
20. Zonia, L. E. Essential role of urease in germination of nitrogen-limited *Arabidopsis thaliana* seeds [Text] / L. E. Zonia, N. E. Stebbins, J. C. Polacco // Plant Physiol. – 1995. – Vol. 107, N 4. – P. 1097-1103.
21. Pedrozo, H. A. A mechanism of adaptation to hypergravity in the statocyst of *Aplysia californica* [Text] / H. A. Pedrozo, Z. Schwartz, M. Luther, D. D. Dean, B. D. Boyan, M. L. Wiederhold // Hear Res. – 1996. – Vol. 102, N 1-2. – P. 51-62.
22. McLean, R. J. C. The ecology and pathogenicity of urease-producing bacteria in the urinary tract [Text] / R. J. C. McLean, J. C. Nickel, K.-J. Cheng, J. W. Costerton // CRC Crit. Rev. Microbiol. – 1988. – Vol. 16, N 1. – P. 37–79.
23. Burne, R. A. Bacterial ureases in infectious diseases [Text] / R. A. Burne, Y.-Y. M. Chen // Microbes and Infection. – 2000. – Vol. 2. – P. 533−542.
24. Collins, C. M. Bacterial ureases: structure, regulation of expression and role in pathogenesis [Text] / M. Collins and S. E. F. D'Orazio // Mol. Microbiol. – 1993. – Vol. 9, N 5. P. 907–913.
25. Follmer, C. Ureases as a target for the treatment of gastric and urinary infections [Text] / C. Folmer // J. Clin. Pathol. – 2010. – Vol. 63, N 5. – P. 424-430.
26. Modolo, L. V. An overview on the potential of natural products as urease inhibitors: a review [Text] / L. V. Modolo, A. X. de Souza, L. P. Horta, D. P. Araujo, A. de Fatima // J. Adv. Res. – 2015. – Vol. 6. – P. 35-44.
27. Kosikowska, P. Urease inhibitors as potential drugs for gastric and urinary tract infections: a patent review [Text] / P. Kosikowska, L. Berlicki // Expert Opin. Ther. Pat. – 2011. – Vol. 21. – P. 945-957.
28. Berlicki, Ł. N-substituted aminomethanephosphonic and aminomethane-P-methylphosphinic acids as inhibitors of ureases [Text] / Ł. Berlicki, M. Bochno, A. Grabowiecka, A. Białas, et al. // Amino Acids. – 2012. – Vol. 42. – P.1937–1945.
29. Xiao, Z.-P. Molecular docking, kinetic study, and structure-activity relationship analysis of quercetin and its analogous as Helicobacter pylori urease inhibitors [Text] / Z.-P. Xiao, X.-D. Wang, Z.-Y. Peng, S. Huang, et al. // Agricult. Food Chem. – 2012. – Vol. 60. – P. 10572-10577.
30. Cun, S.-J. Urease inactivation by an unusual GroES chaperonin [Text] / S.-J. Cun, H.-Z. Sun // Science China Chemistry. – 2014. – Vol. 57, N 6. – P.842–848.
31. Hassan, S. T. S. Plant-derived urease inhibitors as alternative chemotherapeutic agents [Text] / S. T. S. Hassan, M. Zemlicka // Arch. Pharm. Chem. Life Sci. – 2016. Vol. 349. – P. 1–16.
32. Xiao, Z.-P. Synthesis and evaluation of N-analogs of 1,2-diarylethane as *Helicobacter pylori* urease inhibitors [Text] / Z.-P. Xiao, W.-K. Shi, P.-F. Wang, W. Wei, et al. // Bioorganic and Medicinal Chemistry. – 2015. – Vol. 23. – P. 4508–4513.
33. Mazzei, L. Inactivation of urease by 1,4-benzoquinone: chemistry at the protein surface [Text] / L. Mazzei, M. Cianci, F. Musiani, S. Ciurli // Dalton Trans. – 2016. – Vol. 45. – P. 5455-5459.
34. Mazzei, L. Inactivation of urease by catechol: kinetics and structure [Text] / L. Mazzei, M. Cianci, F. Musiani, G. Lente, et al. // J. Inorg. Biochem. – 2017. – Vol.166. – P. 182-189.
35. Zambelli, B. Chemistry of Ni^{2+} in urease: Sensing, trafficking, and catalysis [Text] / D. Zambelli, F. Musiani, S. Benini, S. Ciurli // Accounts Chem. Res. – 2011. – Vol. 44. – P. 520-530.
36. Balasubramanian, A. Crystal structure of the first plant urease from jack bean: 83 years of journey from its first crystal to molecular structure [Text] / A. Balasubramanian, K, Ponnuraj // J. Mol. Biol. – 2010. Vol. 400. – P. 274–283.
37. Jabri, E. The crystal structure of urease from Klebsiella aerogenes [Text] / E. Jabri, M. B. Carr, R. P. Hausinger, P. A. Karplus // Science. – 1995. – Vol. 268, N 5213. – P. 998-1004.
38. Karplus, P.A. 70 years of crystalline urease: what have we learned? [Text] / P. A. Karplus, M. F. Pearson, R. P. Hausinger // Acc. Chem. Res. – 1997. – Vol. 30. – P. 330-337.
39. Ha, N.-C. Supramolecular assembly and acid resistance of *Helicobacter pylori* urease [Text] / N.-C. Ha, S.-T. Oh, J. Y. Sung, et al. // Nature Struct. Biol. - 2001. – Vol. 8. – P. 505-509.
40. Benini, S. A new proposal for urease mechanism based on the crystal structures of the native and inhibited enzyme from Bacillus pasteurii: why urea hydrolysis costs two nickels? [Text] / S. Benini, W. R. Rypniewski, K. S. Wilson, S. Miletti, et al. // Structure. – 1999. – Vol. 7, N 2. – P. 205-216.

DOI: 10.5281/zenodo.1000132

41. Habel, J. E. Structure of Rv1848 (UreA), the *Mycobacterium tuberculosis* urease gamma subunit [Text] / J. E. Habel, E. H. Bursey, B. S. Rho, et al. // Acta Crystallogr. Sect. F Struct. Biol. Cryst. Commun. – 2010. – Vol. 66, N 7. – P. 781-786.
42. Venselaar, H. Homology modelling and spectroscopy, a never-ended love story [Text] / H. Venselaar, R. P. Joosten, B. Vroling, C. A. B. Baakman, et al. // Eur. Biophys. J. – 2010. – Vol. 39. – P. 551-563.
43. Masini, T. Validation of a homology model of *Mycobacterium tuberculosis* DXS: rationalization of observed activities of thiamine derivatives as potent inhibitors of two orthologues of DXS [Text] / T. Masini, B. Lacy, L. Monjas, D. Hawksley, et al. // Org. Biol. chem. – 2015. – Vol. 13. – P. 11263-11277.
44. Ganguly, B. Homology modeling, functional annotation and comparative genomics of outer membrane protein H of *Pasteurella multocida* [Text] / B. Ganguly, K. Tewari, R. Singh // Journal of Theoretical Biology. – 2015. – Vol. 386. – P. 18-24.
45. Benson, D. A. GenBank [Text] / D. A. Benson, I. Karsch-Mizrachi, D. J. Lipman, J. Ostell, D. L. Wheeler // Nucl. Acids Res. – 2007. – Vol. 35, Suppl 1. – P. D21-D25.
46. Altschul, S. F. Basic local alignment search tool [Text] / S. F. Altschul, W. Gish, W. Miller, E. W. Myers, D. J. Lipman // J. Mol. Biol. – 1990. – Vol. 215. - P. 403-410.
47. Altschul, S. F. Gapped BLAST and PSI-BLAST: a new generation of protein database search programs [Text] / S. F. Altschul, T. L. Madden, A. A. Schaeffer, J. Zhang, Z. Zhang, W. Miller, D. J. Lipman // Nucleic Acids Res. – 1997. – Vol. 25. - P. 3389-3402.
48. Rose, P. W. The RCSB protein data bank: integrative view of protein, gene and 3D structural information [Text] / P. W. Rose, A. Prlić, A. Altunkaya, C. Bi et al. // Nucleic Acids Research. – 2017. – Vol. 45. – P. D271-D281.
49. Hooft, R. W. W. Errors in protein structure [Text] / R. W. W. Hooft, G. Vriend, C. Sander, E. E. Abola // Nature. – 1996. – Vol. 381, N 6580. – P. 272-272.
50. Hooft, R. W. W. The PDBFINDER database: A summary of PDB, DSSP and HSSP information with added value [Text] / R. W. W. Hooft, C. Sander, G. Vriend G. // CABIOS/Bioinformatics. – 1996. – Vol. 12. – P. 525-529.
51. Mueckstein, U. Stochastic pairwise alignments [Text] / U. Mueckstein, I. L. Hofacker, P. F. Stadler // Bioinformatics. – 2002. – Vol. 18, Sup. 2. – P. 153-160.
52. Qiu, J. SSALN: an alignment algorithm using structure dependent substitution matrices and gap penalties learned from structurally aligned protein pairs [Text] / J. Qiu, R. Elber // Proteins. – 2006. – Vol. 62. – P. 881–891.
53. Canutescu, A. A. Cyclic coordinate descent: A robotics algorithm for protein loop closure [Text] / A. A. Canutescu, R. L. Jr. Dunbrack // Protein Sci. – 2003. – Vol. 12. – P. 963-972.
54. Canutescu, A. A. A graph-theory algorithm for rapid protein side-chain prediction [Text] / A. A. Canutescu, A. A. Shelenkov, R. L. Jr. Dunbrack // Protein Sci. – 2003. – Vol. 12. – P. 2001-2014.
55. Krieger, E. Assignment of protonation states in proteins and ligands: combining pKa prediction with hydrogen bonding network optimization [Text] / E. Krieger, R. L. Dunbrack, R. W. Hooft, B. Krieger // Methods Mol. Biol. – 2012. – Vol. 819. – P. 405-421.
56. Kreiger, E. Improving physical realism, stereochemistry, and side-chain accuracy in homology modelling: four approaches that perfomed well in CASP8 [Text] / E. Kreiger, K. Joo, J. Lee, et al. // Proteins. – 2009. – Vol. 77, Suppl. 9. – P. 114-122.
57. Krieger, E. Making optimal use of empirical energy functions: force field parameterization in crystal space [Text] / E. Krieger, T. Darden, S. Nabuurs, et al. // Proteins. – 2004. – Vol. 57. – P. 678-683.
58. Krieger, E. Increasing the precision of comparative models with YASARA NOVA - a self-parameterizing force field [Text] / E. Krieger, G. Koraimann, G. Vriend // Proteins. – 2002. – Vol. 47. – P. 393-402.
59. Krieger, E. Fast empirical pKa prediction by Ewald summation [Text] / E. Krieger, J. E. Nielsen, C. A. Spronk, G. Vriend // J. Mol. Graph. Model. – 2006. – Vol. 25, N 4. – P. 481-486.
60. Krieger, E. YASARA View - molecular graphics for all devices - from smartphones to workstations [Text] / E. Krieger, G. Vriend // Bioinformatics. – 2014. – Vol. 30. – P. 2981-2982.
61. Krieger, E. New ways to boost molecular dynamics simulations [Text] / E. Krieger, G. Vriend // J.Comput.Chem. – 2015. – Vol.36. – P. 996-1007.
62. Benkert, P. QMEAN: A comprehensive scoring function for model quality assessment [Text] / P. Benkert, S. C. E. Tosatto, D. Schomburg // Proteins: Structure, Function, and Bioinformatics. - 2008. – Vol. 71, N 1. – P. 261-277.
63. Benkert, P. Towards the estimation of the absolute quality of individual protein structure model [Text] / P. Benkert, M. Basiani, T. Schwede // Bioinformatics. - 2011. – Vol. 27, N 3. – P. 343-350.
64. Benkert, P. QMEAN server for protein model quality estimation [Text] / P. Benkert, M. Kuenzli, T. Schwede // Nucleic Acids Res. – 2009. – Vol. 37. – P. W510-514.
65. Laskowski, R. A. Enhancing the functional annotation of PDB structures in PDBsum using key figures extracted from the literature [Text] / R. A. Laskowski // Bioinformatics. – 2007. – Vol. 23. – P. 1824-1827.
66. Laskowski, R. A. PDBsum: summaries and analyses of PDB structures [Text] / R. A. Laskowski // Nucleic Acids Res. – 2001. – Vol. 29. – P. 221-222.
67. Laskowski, R. A. PDBsum more: new summaries and analyses of the known 3D structures of proteins and nucleic acids [Text] / R. A. Laskowski, V. V. Chistyakov, J. M. Thornton // Nucleic Acids Res. – 2005. – Vol. 33. – P. D266-D268.
68. Laskowski, R. A. PDBsum new things [Text] / R. A. Laskowski // Nucleic Acids Res. – 2009. – Vol. 37. – P. D355-D359.
69. Wallace, A. C. LIGPLOT: a program to generate schematic diagrams of protein-ligand interactions [Text]

DOI: 10.5281/zenodo.1000132

/ A. C. Wallace, R. A. Laskowski, J. M. Thornton // Protein Eng. – 1996. – Vol. 8. – P. 127-134.
70. de Beer, T. A. P. PDBsum additions [Text] / T. A. P. de Beer, K. Berka, J. M. Thornton, R. A. Laskowski // Nucleic Acids Res. – 2014. – Vol. 42. - P. D292-D296.
71. Krissinel, E. Inference of macromolecular assemblies from crystalline state [Text] / E. Krissinel, K. Henrick // J. Mol. Biol. – 2007. – Vol. 372. – P. 774-797.
72. Hornak, V. Comparison of multiple AMBER force field and development of improved protein backbone parameters [Text] / V. Hornak, R. Abel, A. Okur, B. Strockbine, et al. // Proteins. – 2006. – Vol. 65. – P. 712-725.
73. Essman, U. A smooth particle mesh Ewald method [Text] / U. Essman, L. Perera, M. L. Berkowitz, et al. // J. Chem. Phys. B. – 1995. – Vol. 103. – P. 8577-8593.
74. Farrugia, M. A. Analysis of a soluble $(UreD:UreF:UreG)_2$ accessory protein complex and its interactions with *Klebsiella aerogenes* urease by Mass Spectrometry [Text] / M. A. Farrugia1, L. Han, Y. Zhong, J. L. Boer, B. T. Ruotolo, R. P. Hausinger // J. Am. Soc. Mass. Spectrom. – 2013. – Vol. 24, N 9. – P. 1328–1337.
75. Ligabue-Braun, R. Evidence-based docking of the urease activation complex [Text] / R. Ligabue-Braun, R. Real-Guerra, C. R. Carlini, H. Verli // J. Biomol. Struct. Dyn. – 2013. - Vol. 31, N 8. – P. 854–861.
76. Quiroz-Valenzuela, S. The structure of urease activation complexes examined by flexibility analysis, mutagenesis, and small-angle X-ray scattering./ S. Quiroz-Valenzuela, S. C. Sukuru, R. P. Hausinger, L. A. Kuhn, W. T. Heller // Arch. Biochem. Biophys. – 2008. – Vol. 480, 51–57.
77. Fong, Y. H. Structure of UreG/UreF/UreH complex reveals how urease accessory proteins facilitate maturation of *Helicobacter pylori* urease [Text] / Y. H. Fong, H. C. Wonh, M. H. Yuen, P. H. Lau et al. // PLoS Biol. – 2013. – Vol. 11, N 10. – P. 1-16.
78. Lv, J. Structural and functional role of nickel ions in urease by molecular dynamics simulations [Text] / J. Lv, Y. Jiang, Q. Yu. // J. Biol. Inorg. Chem. – 2011. – Vol. 16. – P. 125-135.
79. Roberts, B. P. Wide-open flaps are key to urease activity [Text] / B. P. Roberts, B. R. Miller, A. E. Roitberg, R. M. Merz // J. Am. Chem. Soc. – 2012. – Vol. 134. – P. 9934–9937.
80. Macomber, L. Reduction urease activity by interaction with the flap covering the active site [Text] / L. Macomber, M. S. Minkara, R. P. Hausinger, K. M. Merz // J. Chem. Inf. Model. – 2015. – Vol. 55, N 2. – P. 354-361.
81. Minkara, M. S. Molecular dynamics study of *Helicobacter pylori* urease [Text] / M. S. Minkara, M. N. Ucisik, M. N. Weaver, K. M. Merz, Jr. // J. Chem. Theory Comput. – 2014. – Vol. 10. – P. 1852-1862.

HOMOLOGY MODELING AND MOLECULAR DYNAMICS STUDY OF *MYCOBACTERIUM TUBERCULOSIS* UREASE

Lisnyak Yu. V., Martynov A. V.

Introduction. *M. tuberculosis* urease (MTU) is an attractive target for chemotherapeutic intervention in tuberculosis by designing new safe and efficient enzyme inhibitors. A prerequisite for designing such inhibitors is an understanding of urease's three-dimensional (3D) structure organization. 3D structure of *M. tuberculosis* urease is unknown. When experimental three-dimensional structure of a protein is not known, homology modeling, the most commonly used computational structure prediction method, is the technique of choice. This paper aimed to build a 3D-structure of *M. tuberculosis* urease by homology modeling and to study its stability by molecular dynamics simulations. **Materials and methods.** To build MTU model, five high-resolution X-ray structures of bacterial ureases with three-subunit composition (2KAU, 5G4H, 4UBP, 4CEU, and 4EPB) have been selected as templates. For each template five stochastic alignments were created and for each alignment, a three-dimensional model was built. Then, each model was energy minimized and the models were ranked by quality Z-score. The MTU model with highest quality estimation amongst 25 potential models was selected. To further improve structure quality the model was refined by short molecular dynamics simulation that resulted in 20 snapshots which were rated according to their energy and the quality Z-score. The best scoring model having minimum energy was chosen as a final homology model of 3D structure for *M. tuberculosis*. The final model of MTU was also validated by using PDBsum and QMEAN servers. These checks confirmed good quality of MTU homology model. **Results and discussion.** Homology model of MTU is a nonamer (homotrimer of heterotrimers, $(\alpha\beta\gamma)_3$) consisting of 2349 residues. In MTU heterotrimer, sub-units α, β, and γ tightly interact with each other at a surface of approximately 3000 $Å^2$. Sub-unit α contains the enzyme active site with two Ni atoms coordinated by amino acid residues His347, His349, carbamylated Lys430*, His459, His485, Asp 573, Gly490. Helix-turn-helix motif (residues 524-545) forms a mobile flap that covers the active site and is in closed conformation impeding access to the enzyme active site. The structural stability of MTU model was checked by molecular dynamics simulation in explicit water at 300 K and pH 7,4. During the simulation, root mean square deviations of C_α atoms (RMSD C_α) and root mean square fluctuations (RMSF) of amino acid residues of MTU were monitored for 60 ns. Also, the distance between the loop that covers the active site and the dinickel center was monitored. Analysis of MD trajectory indicate that the enzyme global structure is stable and the flap covering the active center remains in closed state during the simulation time. **Conclusion.** Predicted three-dimensional structure of *M. tuberculosis* urease can be used in the studies of structure-function relationships of the enzyme, in designing new safe and efficient enzyme inhibitors aimed to struggle with infectious diseases promoted by urease activity.

Key words: *Mycobacterium tuberculosis* urease, three-dimensional structure, homology modeling, molecular dynamics simulations

DOI: 10.5281/zenodo.1000132